Research Article

PC4 serves as a negative regulator of skin wound healing in mice

Fengying Liao[1], Long Chen[1], Peng Luo[1], Zhongyong Jiang[1], Zelin Chen[1], Ziwen Wang[1], Chi Zhang[1], Yu Wang[1], Jintao He[1], Qing Wang[1,2], Yawei Wang[1], Lang Liu[1,3], Yu Huang[1,3], Huilan Wang[1,2], Qingzhi Jiang[1,2], Min Luo[1,3], Yibo Gan[1], Yunsheng Liu[1], Yang Wang[1], Jie Wu[1], Wentao Xie[1], Zhuo Cheng[1], Yali Dai[1], Jialun Li[1], Zujuan Liu[1], Fan Yang[1,*] and Chunmeng Shi[1,*]

[1]Institute of Rocket Force Medicine, State Key Laboratory of Trauma, Burns and Combined Injury, Third Military Medical University (Army Medical University), Chongqing 400038, China, [2]Institute of Clinical Medicine, Southwest Medical University, 646000 Luzhou, China and [3]Department of Toxicology, Key Laboratory of Environmental Pollution Monitoring and Disease Control, Ministry of Education, Guizhou Medical University, 550025 Guiyang, China

*Correspondence. Chunmeng Shi, Email: shicm@sina.com; Fan Yang, Email: 956873053@qq.com

Abstract

Background: Human positive cofactor 4 (PC4) was initially characterized as a multifunctional transcriptional cofactor, but its role in skin wound healing is still unclear. The purpose of this study was to explore the role of PC4 in skin wound healing through PC4 knock-in mouse model.

Methods: A PC4 knock-in mouse model (PC4$^{+/+}$) with a dorsal full-thickness wound was used to investigate the biological functions of PC4 in skin wound healing. Quantitative PCR, Western blot analysis and immunohistochemistry were performed to evaluate the expression of PC4; Sirius red staining and immunofluorescence were performed to explore the change of collagen deposition and angiogenesis. Proliferation and apoptosis were detected using Ki67 staining and TUNEL assay. Primary dermal fibroblasts were isolated from mouse skin to perform cell scratch experiments, cck-8 assay and colony formation assay.

Results: The PC4$^{+/+}$ mice were fertile and did not display overt abnormalities but showed an obvious delay in cutaneous healing of dorsal skin. Histological staining showed insufficient re-epithelialization, decreased angiogenesis and collagen deposition, increased apoptosis and decreased cell proliferation in PC4$^{+/+}$ skin. Our data also showed decreased migration rate and proliferation ability in cultured primary fibroblasts from PC4$^{+/+}$ mice *in vitro*.

Conclusions: This study suggests that PC4 might serve as a negative regulator of skin wound healing in mice.

Key words: Wound healing, Skin, PC4, Proliferation, Migration, Positive cofactor 4

Background

Human positive cofactor 4 (PC4) (also known as coactivator p15) and its yeast ortholog Sub1 [1, 2], is a multifunctional nuclear proteins involved in basal transcription [3–6], DNA replication [3, 7], DNA repair [8–10] and chromatin organization [11, 12]. Previous studies demonstrated that PC4 was upregulated in several cancers [13–20]. In addition, PC4 was

reported to be essential for embryonic development and to promote somatic cell reprogramming *in vitro* [21]. However, the role of PC4 in wound healing remains unclear.

As the largest outer barrier, the skin is challenged by a range of external stress factors, such as mechanical damage, resulting in frequent cell and barrier damage [22, 23]. Moreover, skin is one of the ideal organs for studying wound healing because of its accessibility. In this study, a PC4 knock-in transgenic mouse model (PC4^{+/+}) was successfully constructed and delayed wound healing was observed when compared to wild-type (WT) mice. In addition, our histological studies showed insufficient re-epithelialization and decreased angiogenesis and collagen deposition, but increased apoptosis, in PC4^{+/+} mice. Our results suggest that PC4 might play a role in skin wound healing.

Methods

Animals

All C57BL mice aged 6–8 weeks and weighing about 22 g were purchased from the Laboratory Animal Centre of the Army Medical University (Chongqing, China). The experiments were conducted in accordance with the Guidelines for the Care and Use of Laboratory Animals of the Army Medical University (AMU), and the experimental protocols used in this study were approved by the Animal Care Committee of AMU.

Wound model

The mice were anesthetized and shaved. A round full-thickness skin incision with a diameter of 1 cm was made in the middle of the back [24]. After wounding, the wound surface was photographed for the indicated times, and the area of the wound surface was measured with ImageJ (version 1.48) [25].

Generation of a Sub1(PC4) knock-in mouse model

We constructed a 3′-untranslated region endogenous mouse Sub1(PC4) track for a vector containing both the homologous arms (HAs) of the EF1α-mouse Sub1(PC4) cDNA-IRES-eGFP-PolyA knock-in (KI) box to ensure efficient homologous recombination (HR) (Fig. 1a). In the targeting vector, the positive selection marker (Neo) was flanked with LoxP sites. DTA was used for negative selection. The constitutive KI allele was obtained after Cre-mediated recombination. We verified the fidelity of the targeted structures before direct Sanger sequencing of embryonic stem cells (ES cells). Transgenic mice were generated using the standard method (Cyagen Biosciences Inc., China). After drug screening and polymerase chain reaction (PCR) confirmation, ES cell clones with correct HR were expanded and injected into blastocysts, which were then re-implanted into pseudo-pregnant females. To identify F1 mice (the first generation of mice produced by crossbreeding inbred mice) with recombinant alleles, standard PCR screening was performed using primer sets F1-R1 and F2-R1

(Supplementary Fig. 1) to identify the constitutive KI alleles (Fig. 1a).

Cell culture

Newborn PC4^{+/+} or WT C57BL/6 mice were soaked in alcohol for at least 10 minutes. Dorsal full-layer skin samples were collected and moistened with sterile phosphate-buffered saline (PBS) at least thrice. The samples were digested with trypsin (Abcam, USA) at 4°C for 12 hours and the epidermis was discarded. The remaining tissues were cut and digested with 0.25% collagenase I (Thermo Fisher Scientific Inc., USA) at 37°C for 0.5 hours. The digested cells were filtered with a 75 µm cell filter, then the liquid was retained and centrifugally suspended in a normal medium containing 10% fetal bovine serum and 5% CO$_2$ at 37°C. In our experiments, only the cells from passage 2 or 3 were used.

Cell migration assay

Primary fibroblasts from WT and PC4^{+/+} mice were seeded on 6-well plates. When fully confluent, cells were treated with 10 µg/ml Mitomycin C (Sigma-Aldrich, Germany) for 1 hour and washed with PBS twice, then scratched with 200 µl pipettes. Measured the size of the scratch at the beginning of the test and quantified the area of cell migration after 24 hours by Image J software.

Cell proliferation assay

Cell Counting Kit-8 (CCK-8) (MedChemExpress, China) was used to measure cell proliferation ability as per the manufacturer's instructions. In brief, primary fibroblasts from PC4^{+/+} and WT mice were seeded and cultured in 96-well plates at a density of 5×10^3 cells/well. Each cell type was divided into 4 time points (12, 24, 48 and 72 hours) with 6 replicates at each time point. At the end of culture the CCK-8 reagent was added and the cells were cultured for 2 hours at 37°C. Cell viability was measured at a wavelength of 450 nm (OD450).

Colony formation assay

For the colony formation assay, primary fibroblasts from PC4^{+/+} and WT mice were inoculated into six-well plates at a density of 1×10^3 cells/well. The medium was changed twice a week, and cells were cultured for 2 weeks until colonies were clearly visible. The colonies were washed at least twice, fixed with methanol for 15 minutes, and stained with crystal violet for 10 minutes. Colonies with >50 cells were counted.

Hematoxylin and eosin staining

Skin samples carrying the wound bed and those 1–2 mm outside the wound were collected at 3, 7, 10 and 14 days after injury (*n* = 3). Samples were fixed with 4% paraformaldehyde, embedded in paraffin and stained with hematoxylin and eosin at indicated time point. The sample was taken from different mice.

Real-time quantitative PCR

Total RNA was extracted using Trizol (Cwbiotech, China). cDNA synthesis was performed following the manufacturer's protocol (Maxima First Strand cDNA Synthesis Kit, Thermo Scientific Inc, K1671). Real-time PCR (RT-PCR) was carried out using a SYBR Green qPCR master mix (Takara, China) according to the manufacturer's protocol. Relative threshold cycle method was used to ascertain the gene expression levels of every gene. Glyceraldehyde 3-phosphate dehydrogenase was used as an internal control. The primers used for RT-qPCR are listed in Supplementary Table 1.

Western blot analysis

Primary fibroblasts from PC4$^{+/+}$ and WT mice were collected, washed and lysed with a lysis buffer (Cell Signaling Technology, USA) supplemented with protease inhibitor cocktail (Thermo Fisher Scientific Inc.) for 0.5 hours on ice. Total protein was quantitated with a bicinchoninic acid assay kit (Thermo Fisher Scientific Inc.). Each sample was denatured with a loading buffer (Beyotime, China), separated by electrophoresis on a 12% gel and transferred onto polyvinylidene fluoride membranes (Millipore, USA). The membranes were blocked with an animal-free blocking solution (Cell Signaling Technology) and incubated with PC4 primary antibody (11 000, ab84459, Abcam) for 16 hours at 4°C. The membranes were washed thrice with Tris-Buffered Saline Tween-20 (TBST) (5 minutes each wash) and incubated for 1–2 hours with horseradish peroxidase-linked secondary antibody (Beyotime) at 25°C. The intensity of bands was visualized and determined using an enhanced chemiluminescence detection system (Bio-Rad Laboratories). Images were quantified with ImageJ software. Actin was used as a loading control. PC4/actin shows relative expression level of PC4 protein.

Immunohistochemical staining

Paraffin-embedded tissue sections were dewaxed, rehydrated and immersed in tris/ethylenediaminetetraacetic acid (pH 9.0) for 15 minutes at 98°C for antigen retrieval. The slides were incubated with PC4 primary antibody overnight at 4°C. The slides were washed thrice with PBS (5 minutes each time), incubated with a biotinylated secondary antibody for 1 hour at 37°C and then detected with 3,3′-diaminobenzidine substrate. The ratio of target protein-positive nuclei to
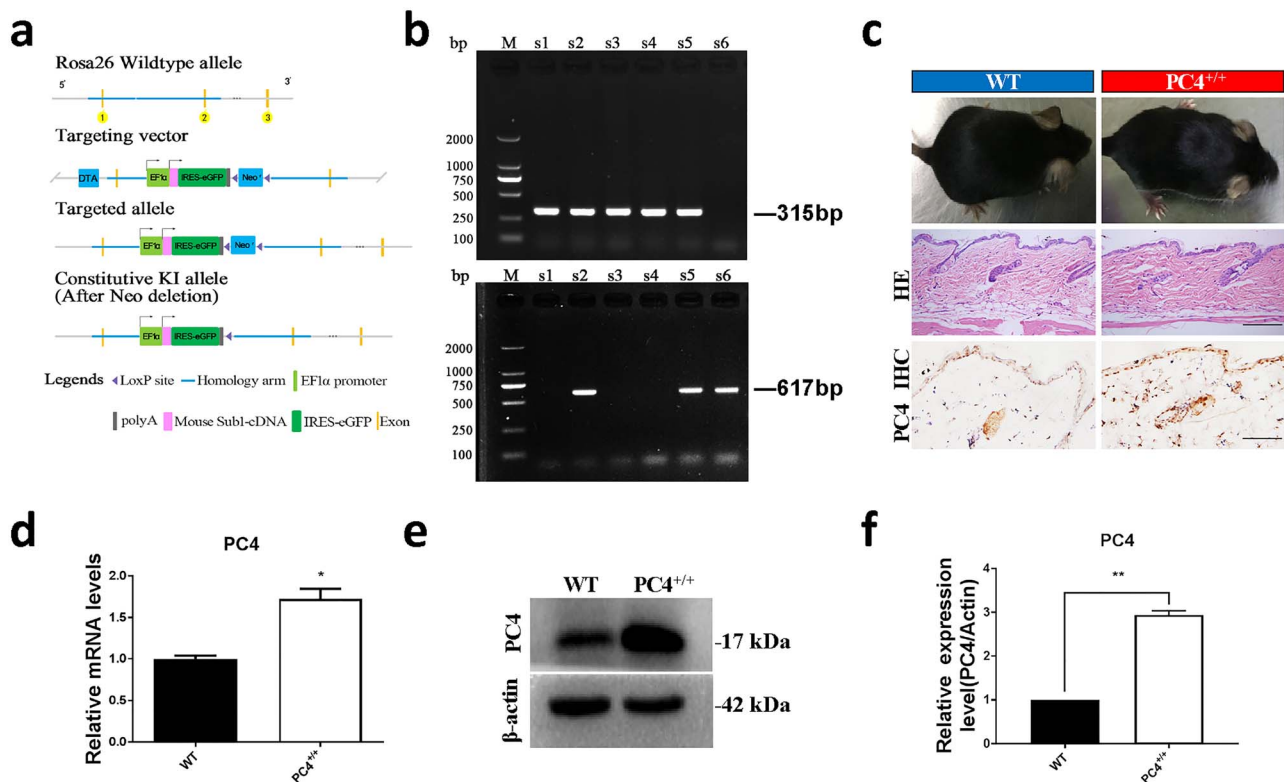
Figure 1. Construction and identification of PC4 knock-in mouse model. **(a)** Strategy used to generate a PC4 knock-in mouse model in C57BL/6 mice. **(b)** PCR genotyping of mice. Genomic DNA isolated from tail snips was digested with BamHI and separated on an agarose gel. **(c)** General comparison between WT and PC4$^{+/+}$ mice using hematoxylin and eosin-stained sections of skin. Skin samples were analysed for the localization of PC4 protein by immunohistochemistry. Scale bar = 100 μm. RT-PCR **(d)** and Western blot **(e)** analysis for the levels of PC4 in the skin from WT and PC4$^{+/+}$ mice. **(f)** Actin was used as a loading control. Ratio of PC4/actin shows relative expression level of PC4 protein. All data indicate the comparison between WT and PC4$^{+/+}$ by independent samples *t*-test, and all data indicate with the mean ± SD; *$p < 0.05$, **$p < 0.01$. *PC4* human positive cofactor 4, *PC4$^{+/+}$* PC4 knock-in mouse model, *PCR* polymerase chain reaction, *WT* wild-type, *SD* standard deviation

DAPI-positive nuclei in 3 microscopic fields per group was used for quantification by ImageJ software. Antibodies used for immunohistochemical staining were: Ki67 (1:200, ab15580, Abcam), CD31 (1:200, ab28364, Abcam), α-smooth muscle actin (1:200, ab32575, Abcam) and terminal deoxynucleotidyl transferase dUTP nick end labelling (TUNEL) (1:200, ab66110, Abcam), while secondary antibodies to different IgG species were conjugated to Alexa Fluor 594 (red) or Alexa Fluor 488 (green) (1500 for all, Invitrogen).

Statistical analysis

P values were calculated with the Student's *t*-test (two-sided) or two-way analysis of variance [26]. GraphPad Prism 8.0 was used for data analysis. All data are presented as mean ± standard deviation.

Results

Construction and identification of PC4 knock-in transgenic mice

To generate a PC4 knock-in transgenic mouse model, an EF1α-mouse Sub1 cDNA-IRES-eGFP-PolyA cassette was cloned into the intron 1 of Rosa26. Mouse genomic fragments containing HAs were amplified from the bacterial artificial chromosome (BAC) clone using high-fidelity *Taq* and sequentially assembled into a targeting vector together with recombination sites (Fig. 1a). To obtain Sub1 homozygous mice (PC4$^{+/+}$), we crossed a heterozygous male mouse with 3 heterozygous female mice in a cage, and designed primers to identify their offspring (Supplementary Fig. 1). The positive homozygous mice had an mutant type (MT) band of 315 bp (Fig. 1b: a1, a3, a4); the WT mice had a WT band of 617 bp (a6 in Fig. 1b), while the positive heterozygous mice had both 315 and 617 bp bands (Fig. 1b: a2, a5). During breeding,
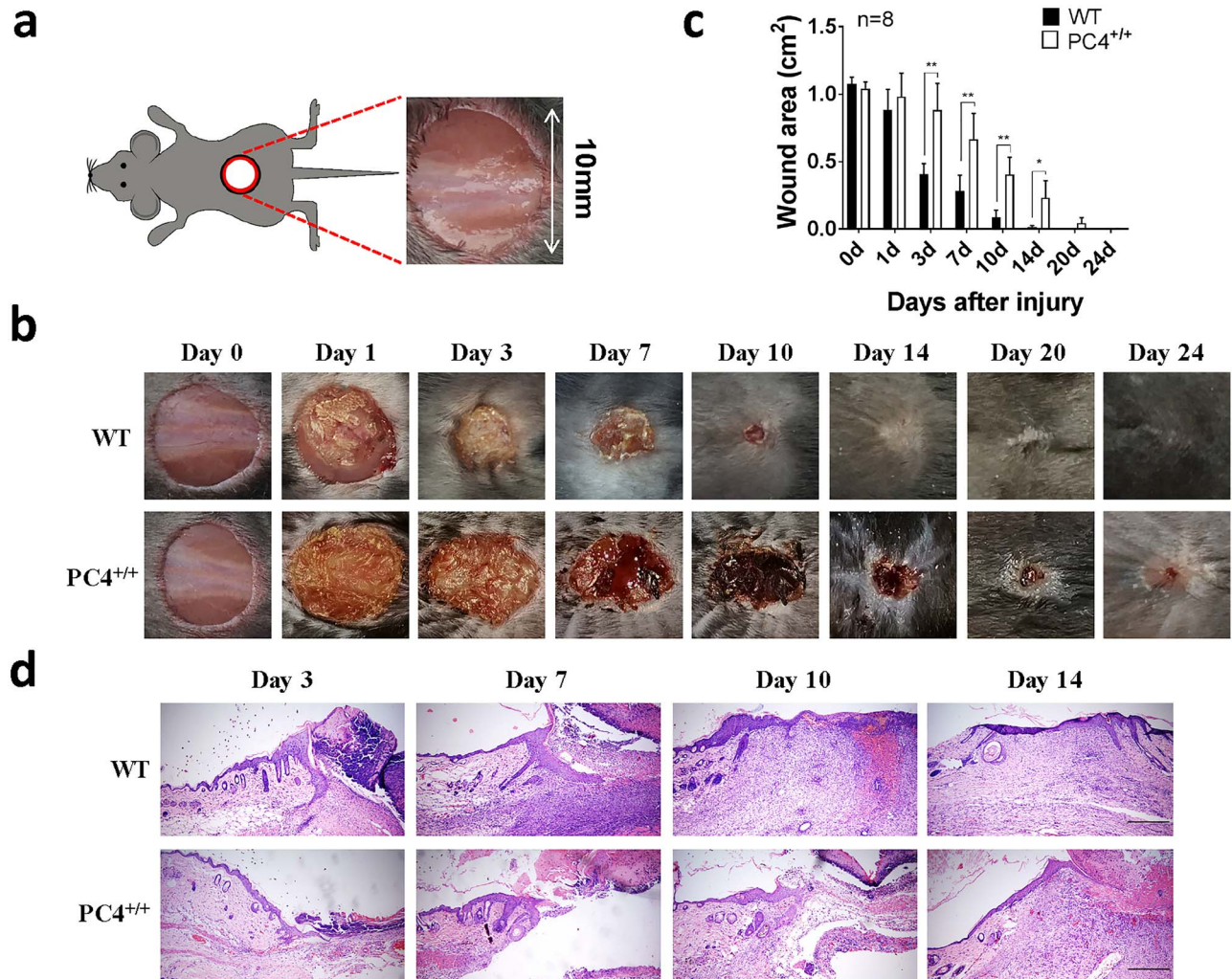
Figure 2. Overexpression of PC4 inhibits wound healing *in vivo*. **(a)** Schematic of the wound healing model. **(b)** Representative images of the skin wound healing for the indicated times (*n* = 8 per group). **(c)** Quantification of the wound areas was performed using *Image* J software. Data represented the means ± SD, **p* < 0.05, ***p* < 0.01. *P* values were calculated with two-way ANOVA. **(d)** Pathological studies confirmed that delayed healing in PC4$^{+/+}$ mice during the granulation tissue maturation process. Representative images of hematoxylin and eosin-stained skin sections from biopsies on days 3, 7, 10 and 14 in WT and PC4$^{+/+}$ mice; *n* = 3 mice per group. Scale bar = 200 μm. *PC4* human positive cofactor 4, *SD* standard deviation, *ANOVA* analysis of variance, *PC4$^{+/+}$* PC4 knock-in mouse model, *WT* wild-type
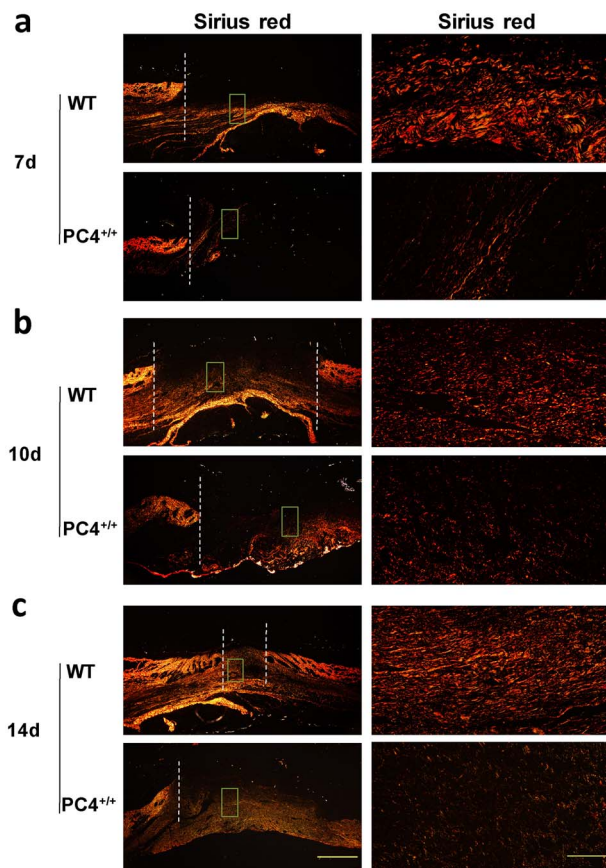
Figure 3. PC4 overexpression decreases collagen deposition and maturation in wounds. Sirius red staining demonstrates the increased collagen deposition and maturation in the wound areas on: **(a)** day 7, **(b)** day 10 and **(c)** day 14. The white dotted line represents the wound edge, while the image on the right is an enlarged image of the box on the left. Scale bar = 200 μm (left) and 100 μm (right). *PC4* human positive cofactor 4

size and sex distribution were proportional to the expected Mendelian pattern, suggesting that the Sub1 KI allele did not have any major phenotypic alterations (Fig. 1c; Supplementary Fig. 2a). PC4 expression was substantially increased in the dermis and epidermis of transgenic mice (Fig. 1c). In addition, we observed that PC4 protein and mRNA levels were significantly higher in primary skin fibroblasts from PC4$^{+/+}$ mice compared WT mice (Fig. 1d, e, f).

Overexpression of PC4 delays wound healing *in vivo*
We made a uniform 10 mm incision in the skin and evaluated cutaneous wound healing by comparing the degree of wound closure between PC4$^{+/+}$ and WT mice (Fig. 2a) to investigate the role of PC4 in skin wound healing *in vivo*. PC4$^{+/+}$ mice showed a significant delay in wound closure from day 3 to 14 compared to WT mice (Fig. 2b, c). Delayed wound healing in PC4$^{+/+}$ mice was observed through pathological studies (Fig. 2d). In contrast, PC4$^{+/+}$ mice showed delayed epidermal and dermal maturation. Abundant cells (including red blood and inflammatory cells) and numerous capillaries observed were indicative of immature granulation tissue (Fig. 2d). Re-epithelialization on days 10 and 14 in PC4$^{+/+}$

mice was insufficient compared to that in WT mice (Supplementary Fig. 2b). Compared with WT mice, PC4$^{+/+}$ mice showed an obviously decreased area of granulation tissue (Supplementary Fig. 2c).

Overexpression of PC4 inhibits collagen deposition and maturation in wounds
Collagen fiber deposition and remodeling are important processes for granulation tissue repair. On days 7, 10 and 14 after injury, the dermis of the normal skin near the wounded surface showed bright Sirius red staining (Fig. 3a, b, c). On day 14, the dermal collagen fibers of WT wounds showed a typical network of crosslinked fibers to maintain skin elasticity and tension (Fig. 3c). On day 10 after injury, moderate deposition of collagen was observed as red staple fibers. From day 7–14 post-injury, collagen formation in PC4$^{+/+}$ mice was lower than that in WT mice, as was evident from Sirius red staining intensity, and the fibers were disordered, thinner, shorter, greener and less red. On day 14, the granulation tissue collagen fibers of WT, but not PC4$^{+/+}$, mice matured into a network, indicating that the collagen network of PC4$^{+/+}$ mice matured later (Fig. 3c).
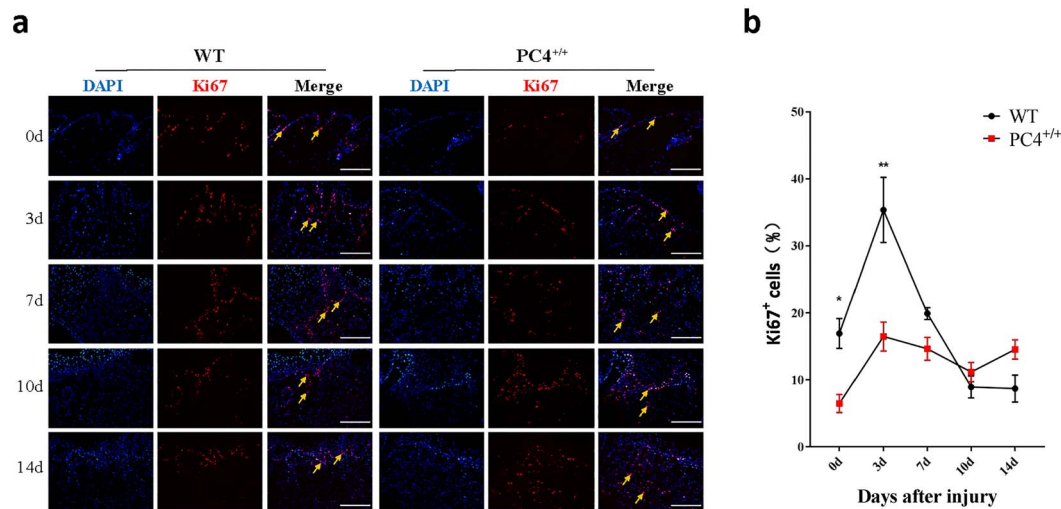
Overexpression of PC4 expression inhibits cell proliferation and promotes cell apoptosis in wounds
Proliferation and apoptosis are prerequisites for wound healing [27, 28]. In general, cell proliferation and apoptosis are maintained at a stable level in normal skin. Ki67 and TUNEL immunofluorescence staining were used to detect the accumulation of proliferating and apoptotic cells in skin wounds. Noticeably increased proliferation was observed in the wound area of WT mice on days 3 and 7 compared to that in PC4$^{+/+}$ mice, as confirmed by Ki67-positive cells (Fig. 4a, b). The quantification of TUNEL staining revealed a substantial increase in the number of apoptotic cells in PC4$^{+/+}$ mice on days 3 and 7 compared with that in WT mice (Fig. 5).

Overexpression of PC4 reduces angiogenesis and cell migration in wounds
Neovascularization is critical for efficient wound healing [29] and essential for the supply of nutrients and the maintenance of oxygen homeostasis, thereby facilitating cell proliferation and tissue regeneration [30]. In this study, CD31 immunofluorescence staining was performed to detect neovascularization or new blood vessel formation in wounded skin samples. Our results showed that more neovascularization was observed in the wounded region on days 3 and 7 in WT mice (Fig. 6a). Neovascularization began to decrease on day 10 and was near normal by day 14. In contrast, no substantial increase of neovascularization was observed in PC4$^{+/+}$ mice by day 3. However, there was continuous increase of neovascularization by days 10 and 14 in PC4$^{+/+}$ mice.

Alpha smooth muscle actin (α-SMA) is important for cell migration to promote wound contraction during healing. The obviously increased α-SMA was observed in the wound area

a

b

Figure 4. Overexpression of PC4 inhibits cell proliferation in wounds **(a)** Ki67 immunofluorescence staining revealed cell proliferation at the healing sites of skin wounds on days 0, 3, 7, 10 and 14. Scale bar = 100 μm. Arrows show representative Ki67-positive/DAPI-positive cells. **(b)** The relative quantitative changes in Ki67-positive cells were observed in the skin wound healing sites after 0, 3, 7, 10 and 14 days in WT and PC4$^{+/+}$ mice. *$p < 0.05$, **$p < 0.01$. *P* values were calculated with two-way ANOVA. *PC4* human positive cofactor 4, *WT* wild-type, *ANOVA* analysis of variance
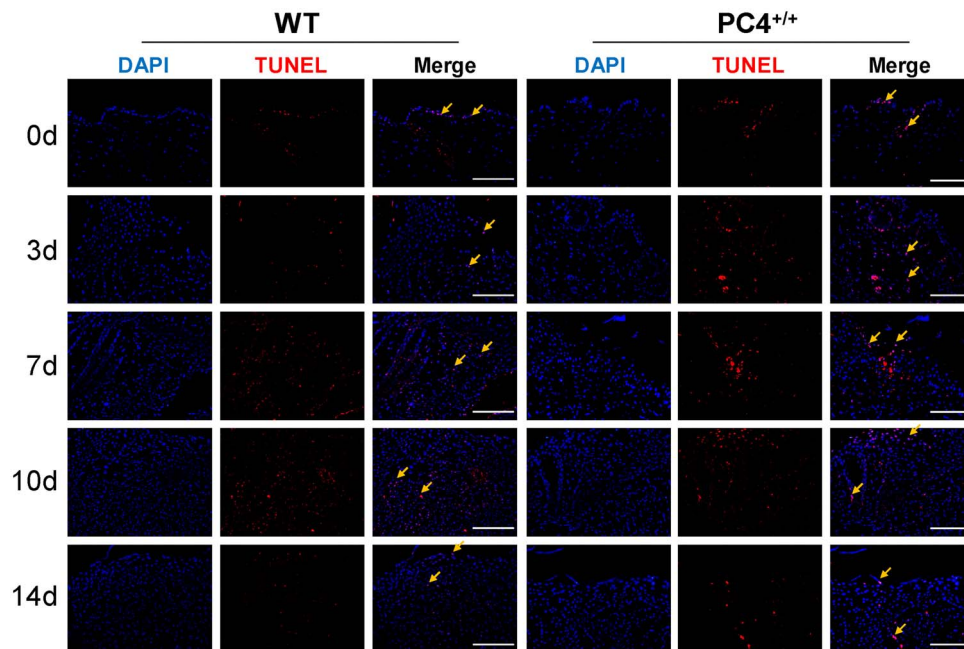
Figure 5. Overexpression of PC4 promotes cell apoptosis in wounds. TUNEL immunofluorescence staining showed cell apoptosis at the healing sites of skin wounds on days 0, 3, 7, 10 and 14. Scale bar = 100 μm. Arrows show representative TUNEL-positive/DAPI-positive cells. *PC4* human positive cofactor 4, *TUNEL* Transferase dUTP nick end labelling

from day 3 to 10 in both WT and PC4$^{+/+}$ mice; however, α-SMA-positive cells were significantly lower in PC4$^{+/+}$ mice than in WT mice, as determined by immunofluorescence staining in the wounded region (Fig. 6b).

Overexpression of PC4 in skin primary fibroblasts inhibits cell migration and proliferation *in vitro*

To further investigate the function of PC4 for cell migration and proliferation, skin primary fibroblasts were taken from mice for *in vitro* studies. Scratch test showed that overexpression of PC4 in primary skin fibroblasts decreased their migration ability (Fig. 7a, b). CCK-8 assays and colony formation

assays showed that the overexpression of PC4 in primary fibroblasts resulted in significantly reduced proliferation *in vitro* (Fig. 7c, d).

Discussion

Skin repair is a complex process, and the cellular and molecular mechanisms underlying wound healing are still not completely clear [31]. Thus, it is important to identify and screen new repair-related genes for further understanding the healing process. In this study, we proposed, for the first time, the role of PC4 involved in wound healing. With the PC4
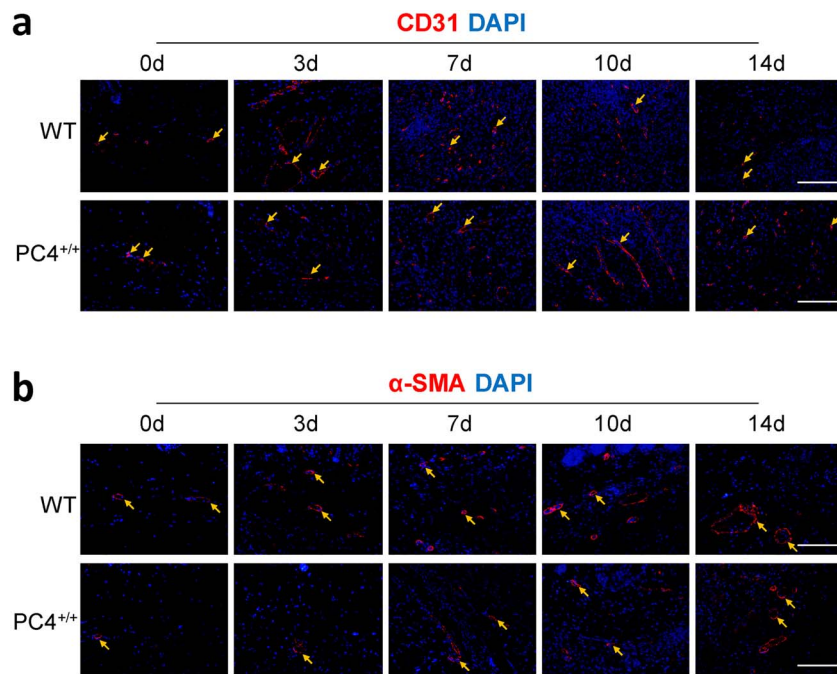
Figure 6. Overexpression of PC4 reduces angiogenesis and cell migration in wounds. **(a)** CD31 (red) and DAPI (blue) expression was shown in the representative images of WT and PC4$^{+/+}$ mice after 0–14 days after trauma. Scale bar = 100 μm. Arrows show representative CD31-positive/DAPI-positive cells. **(b)** α-SMA (red) and DAPI (blue) expression was shown in the representative images of WT and PC4$^{+/+}$ mice after 0 to 14 days after trauma. Scale bar = 100 μm. Arrows show representative α-SMA-positive/DAPI-positive cells. *PC4* human positive cofactor 4, *WT* wild-type, *α-SMA* alpha smooth muscle actin
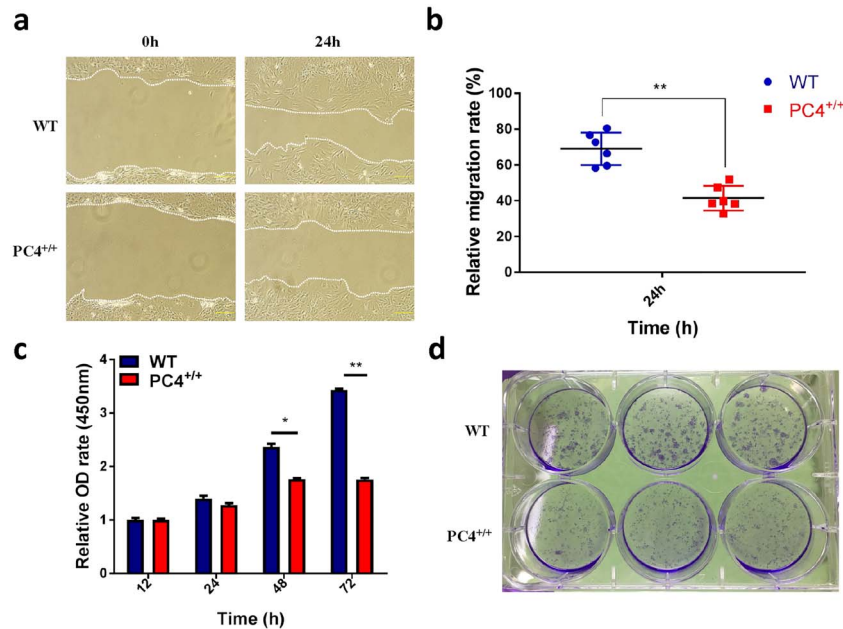
Figure 7. Overexpression of PC4 inhibits cell migration and proliferation *in vitro*. The migration and proliferation of primary fibroblasts derived from PC4$^{+/+}$ mice decreased. **(a)** Images of primary fibroblasts after 24 hours from the initial migration test. Yellow bar: 200 μm. **(b)** Scatter diagram quantifying the relative migration area. Each sample was measured 6 times at the indicated time point. Each experiment was repeated thrice. P values were calculated with t-text. **(c)** Proliferation was measured by CCK-8 assays. *P* values were calculated with two-way ANOVA. **(d)** Clone formation assay was performed with WT and PC4$^{+/+}$ primary fibroblasts. *$p < 0.05$, *$p < 0.01$. *PC4* human positive cofactor 4, *PC4$^{+/+}$* PC4 knock-in mouse model, *CCK-8* cell counting kit-8, *ANOVA* analysis of variance

knock-in mouse model, we first demonstrated that the skin of PC4$^{+/+}$ mice showed a lower amount of granulation tissue and slower re-epithelialization during healing than the skin of WT mice. Our data suggest that PC4$^{+/+}$ attenuates fibroblast proliferation and migration *in vivo* and *in vitro*. In our model, PC4 overexpression promoted apoptosis and delayed

neovascularization. The above results have enriched the understanding of wound healing. Furthermore, PC4$^{+/+}$ mice showed no significant differences in blood routine, thymus, lymph node and spleen biopsy compared with WT mice during wound healing, and the infiltrated immune cells with CD11b (a specific marker of granulocytes and macrophages) and F4/80 (a specific marker of macrophages) also showed no significant differences between the 2 types of mice during healing, which suggests that overexpression of PC4 in the body might not cause systemic changes that affect wound healing.

PC4 was thought as a transcription coactivator with highly conserved sequence among mouse, rat, human, and yeast [4,5]. As a multifunctional nuclear transcription cofactor, PC4 plays an important role in the regulation of embryonic development [32, 33], tumorigenesis [13] and other processes. At present, the regulatory mechanism of PC4 has not been clarified. Previous studies have revealed that PC4 regulates cellular behavior through multiple pathways, including basic transcription [4, 6, 34, 35] and epigenetic modifications [12, 17, 36]. In this study, we demonstrated that PC4 might participate in skin wound healing through PC4 knock-in mice, but in-depth mechanisms remain to be clarified. Because loss of PC4 expression leads to lethality in early embryos, the skin tissue conditional PC4 knock-out and conditional PC4 knock-in models will be helpful to further understand the functions and mechanisms of PC4 during skin wound healing.

Conclusions

In summary, PC4 negatively regulates wound healing in transgenic mice, suggesting that PC4 might play a role in tissue homeostasis and repair.

Supplementary data

Supplementary data is available at *Burns* & *Trauma Journal* online.

Funding

Availability of data and materials

The datasets used and/or analysed in the current study are available from the corresponding author upon reasonable request.

Author contributions

CS and FL designed, carried out and analysed the data from most experiments and wrote the manuscript along with the other co-authors. CS and FY conceived and supervised the study. LC, PL and ZC revised the manuscript. ZJ, ZW, CZ, YW, JH and QW performed experiments. YW, LL, YH, HW, QJ, ML, YG, YL, YW, JW, WX, ZC, JL and YD analysed and interpreted data from experiments. All authors discussed the results and commented on the manuscript.

Ethics approval and consent to participate

The experiments were conducted in accordance with the Guidelines for the Care and Use of Laboratory Animals of the Army Medical University (AMU), and the experimental protocols used in this study were approved by the Animal Care Committee of AMU.

Conflict of interest

None declared.

Acknowledgements

References

1. Ge H, Roeder RG. Purification, cloning, and characterization of a human coactivator, PC4, that mediates transcriptional activation of class II genes. *Cell*. 1994;78:513–23.

2. Kretzschmar M, Kaiser K, Lottspeich F, Meisterernst M. A novel mediator of class II gene transcription with homology to viral immediate-early transcriptional regulators. *Cell*. 1994;78:525–34.

3. Garavís M, Calvo O. Sub1/PC4, a multifaceted factor: from transcription to genome stability. *Curr Genet*. 2017;63: 1023–35.

4. Wang Z, Roeder RG. DNA topoisomerase I and PC4 can interact with human TFIIIC to promote both accurate termination and transcription reinitiation by RNA polymerase III. *Mol Cell*. 1998;1:749–57.

5. Malik S, Guermah M, Roeder RG. A dynamic model for PC4 coactivator function in RNA polymerase II transcription. *Proc Natl Acad Sci USA*. 1998;95:2192–7.

6. Calvo O, Manley JL. The transcriptional coactivator PC4/Sub1 has multiple functions in RNA polymerase II transcription. *EMBO J*. 2005;24:1009–20.

7. Akimoto Y, Yamamoto S, Iida S, Hirose Y, Tanaka A, Hanaoka F, *et al.* Transcription cofactor PC4 plays essential roles in collaboration with the small subunit of general transcription factor TFIIE. *Genes Cells*. 2014;19:879–90.

8. Gao J, Zybailov BL, Byrd AK, Griffin WC, Chib S, Mackintosh SG, *et al.* Yeast transcription co-activator Sub1 and its human homolog PC4 preferentially bind to G-quadruplex DNA. *Chem Commun (Camb)*. 2015;51:7242–44.

9. Huang J, Zhao Y, Liu H, Huang D, Cheng X, Zhao W, *et al.* Substitution of tryptophan 89 with tyrosine switches the DNA binding mode of PC4. *Sci Rep*. 2015;5:8789.

10. Mortusewicz O, Evers B, Helleday T. PC4 promotes genome stability and DNA repair through binding of ssDNA at DNA damage sites. *Oncogene*. 2016;35:761–70.

11. Sancar C, Ha N, Yilmaz R, Tesorero R, Fisher T, Brunner M, *et al.* Combinatorial control of light induced chromatin remodeling and gene activation in Neurospora. *PLoS Genet*. 2015;11: e1005105.

12. Das C, Hizume K, Batta K, Kumar BR, Gadad SS, Ganguly S, *et al.* Transcriptional coactivator PC4, a chromatin-associated protein, induces chromatin condensation. *Mol Cell Biol*. 2006;26:8303–15.

13. Shi C, Mai Y, Zhu Y, Cheng T, Su Y. Spontaneous transformation of a clonal population of dermis-derived multipotent cells in culture. *In Vitro Cell Dev Biol Anim*. 2007;43:290–6.

14. Peng Y, Yang J, Zhang E, Sun H, Wang Q, Wang T, *et al.* Human positive coactivator 4 is a potential novel therapeutic target in non-small cell lung cancer. *Cancer Gene Ther*. 2012;19: 690–6.

15. Chen L, Du C, Wang L, Yang C, Zhang JR, Li N, *et al.* Human positive coactivator 4 (PC4) is involved in the progression and prognosis of astrocytoma. *J Neurol Sci*. 2014;346: 293–8.

16. Luo P, Tan X, Luo S, Wang Z, Long L, Wang Y, *et al.* An NIR-Fluorophore-based inhibitor of SOD1 induces apoptosis by targeting transcription cofactor PC4. *Adv Ther (Weinh)*. 2019;2:1800148.

17. Luo P, Zhang C, Liao F, Chen L, Liu Z, Long L, *et al.* Transcriptional positive cofactor 4 promotes breast cancer proliferation and metastasis through c-Myc mediated Warburg effect. *Cell Commun Signal*. 2019;17:36.

18. Luo P, Jiang Q, Fang Q, Wang Y, Wang Z, Yang J, *et al.* The human positive cofactor 4 promotes androgen-independent prostate cancer development and progression through HIF-1α/β-catenin pathway. *Am J Cancer Res*. 2019;9: 682–98.

19. Li W, Hou JZ, Niu J, Xi ZQ, Ma C, Sun H, *et al.* Akt1 inhibition promotes breast cancer metastasis through EGFR-mediated β-catenin nuclear accumulation. *Cell Commun Signal*. 2018;16:82.

20. Du Z, Luo Q, Yang L, Bing T, Li X, Guo W, *et al.* Mass spectrometric proteomics reveals that nuclear protein positive cofactor PC4 selectively binds to cross-linked DNA by a transplatinum anticancer complex. *J Am Chem Soc*. 2014;136: 2948–51.

21. Jo J, Hwang S, Kim HJ, Hong S, Lee JE, Lee SG, *et al.* An integrated systems biology approach identifies positive cofactor 4 as a factor that increases reprogramming efficiency. *Nucleic Acids Res*. 2016;44:1203–15.

22. Kurita M, Araoka T, Hishida T, O'Keefe DD, Takahashi Y, Sakamoto A, *et al.* In vivo reprogramming of wound-resident cells generates skin epithelial tissue. *Nature*. 2018;561: 243–7.

23. Eming SA, Martin P, Tomic-Canic M. Wound repair and regeneration: mechanisms, signaling, and translation. *Sci Transl Med*. 2014;6:265sr6.

24. Dekoninck S, Blanpain C. Stem cell dynamics, migration and plasticity during wound healing. *Nat Cell Biol*. 2019;21: 18–24.

25. Miura T, Kawakami K, Kanno E, Tanno H, Tada H, Sato N, *et al.* Dectin-2-mediated Signaling leads to delayed skin wound healing through enhanced Neutrophilic inflammatory response and neutrophil extracellular trap formation. *J Invest Dermatol*. 2019;139:702–11.

26. Liang G, Fu W, Wang K. Analysis of t-test misuses and SPSS operations in medical research papers. *Burns Trauma*. 2019;7:31.

27. Ma T, Fu B, Yang X, Xiao Y, Pan M. Adipose mesenchymal stem cell-derived exosomes promote cell proliferation, migration, and inhibit cell apoptosis via Wnt/β-catenin signaling in cutaneous wound healing. *J Cell Biochem*. 2019;**120**:10847–54.

28. Justet C, Hernández JA, Torriglia A, Chifflet S. Fast calcium wave inhibits excessive apoptosis during epithelial wound healing. *Cell Tissue Res*. 2016;365:343–56.

29. Duscher D, Maan ZN, Whittam AJ, Sorkin M, Hu MS, Walmsley GG, *et al.* Fibroblast-specific deletion of hypoxia inducible Factor-1 critically impairs murine cutaneous neovascularization and wound healing. *Plast Reconstr Surg*. 2015;136: 1004–13.

30. Icli B, Nabzdyk CS, Lujan-Hernandez J, Cahill M, Auster ME, Wara AK, *et al.* Regulation of impaired angiogenesis in diabetic dermal wound healing by microRNA-26a. *J Mol Cell Cardiol*. 2016;91:151–9.

31. Rodrigues M, Kosaric N, Bonham CA, Gurtner GC. Wound healing: a cellular perspective. *Physiol Rev*. 2019;99:665–706.

32. Iacopetti P, Barsacchi G, Tirone F, Cremisi F. Expression of the PC4 gene in the developing rat nervous system. *Brain Res*. 1996;**707**:293–7.

33. Pröls F, Loser B, Marx M. Differential expression of osteopontin, PC4, and CEC5, a novel mRNA species, during in vitro angiogenesis. *Exp Cell Res*. 1998;239:1–10.

34. Malik S, Guermah M, Roeder RG. A dynamic model for PC4 coactivator function in RNA polymerase II transcription. *Proc Natl Acad Sci USA*. 1998;95:2192–7.

35. Tavenet A, Suleau A, Dubreuil G, Ferrari R, Ducrot C, Michaut M, *et al.* Genome-wide location analysis reveals a role for Sub1 in RNA polymerase III transcription. *Proc Natl Acad Sci USA*. 2009;**106**:14265–70.

36. Das C, Gadad SS, Kundu TK. Human positive coactivator 4 controls heterochromatinization and silencing of neural gene expression by interacting with REST/NRSF and CoREST. *J Mol Biol*. 2010;397:1–12.